Available online at www.sciencedirect.com
SCIENCE DIRECT®
Journal of Steroid Biochemistry & Molecular Biology 89–90 (2004) 55–59
The Journal of Steroid Biochemistry & Molecular Biology
www.elsevier.com/locate/jsbmb

Structural investigation of the ligand binding domain of the zebrafish VDR in complexes with 1α,25(OH)$_2$D$_3$ and Gemini: purification, crystallization and preliminary X-ray diffraction analysis☆

Fabrice Ciesielski[a], Natacha Rochel[a], Andre Mitschler[a], Alexander Kouzmenko[b], Dino Moras[a,*]

[a] *Département de Biologie et de Génomique Structurales, IGBMC, CNRS/INSERM/Université Louis Pasteur, Parc d'Innovation BP10142, 67404 Illkirch cedex, France*
[b] *Laboratory of Molecular Signaling, Institute of Molecular and Cellular Biosciences, University of Tokyo, 1-1-1 Yayoi, Bunkyo-ku, Tokyo, Japan*

Abstract

The nuclear receptor of Vitamin D can be activated by a large number of agonist molecules with a wide spectrum in their stereochemical framework. Up to now most of our structural information related to the protein–ligand complex formation is based on an engineered ligand binding domain (LBD) of the human receptor. We now have extended our database, using a wild-type LBD from zebrafish that confirms the previously reported results and allows to investigate the binding of ligands that induce significant conformational changes at the protein level.

Keywords: VDR; LBD; Crystal structure; 1α,25(OH)$_2$D$_3$; Gemini; Purification; Crystallization

1. Introduction

The Vitamin D nuclear receptor (VDR) is a member of the nuclear receptor superfamily [1], which are ligand-dependent transcriptional regulator controlling cell growth and differentiation, homeostasis and several physiological processes. Ligand binding induces a conformational change of the AF-2 helix at the C-ter of the ligand binding domain (LBD) that allows the recruitment of coactivator from the p160 [2] or the DRIP/TRAP [3] families. The active form of Vitamin D, 1α,25(OH)$_2$D$_3$, regulates calcium and phosphate metabolism, cell differentiation and has immunosuppressive effects [4]. Most analogs of 1α,25(OH)$_2$D$_3$ developed to date are modified at their side chain. They were synthesized with the goal to improve the biological profile of the natural ligand with decreased hypercalcemic effects for therapeutic application.

VDRs have been characterized from mammals [5–7], birds [8], *Xenopus laevis* [9], *Paralichtus olivaceus* [10], zebrafish (GenBank accession number AAF21427) and recently from lampreys [11]. Sequence analysis of the VDR subfamily members reveals that VDR present a large insertion domain, poorly conserved between VDRs species, at the N-terminal region of the LBD in the peptide connecting helices H1–H3. Secondary structure prediction programs reveal that this region is not structured. In order to stabilize the overall structure of the hVDR, we have engineered a hVDR LBD mutant (hVDRΔ) by deleting 50 residues in the region connecting helices H1–H3. This VDR mutant stabilized the protein by lowering the number of conformations adopted by the insertion region. The biological properties (binding, transactivation) of the mutant protein are similar to those of the wild-type [12,13].

This hVDRΔ construct let us to crystallize several complexes with agonist ligands [12,14]. In all these complexes, the overall conformation of the protein is identical and adopts the agonist conformation. The interaction between the ligands and the receptor involve both hydrophobic and electrostatic interactions. All the ligands fit into the mold of the ligand binding site (Fig. 1). The 20-epi analogs make several specific contacts with the protein as a consequence of the different path adopted by the aliphatic chain.

Packing constraints of the unique crystal form obtained discriminates complexes with conformational changes near the ligand pocket. In order to crystallize new complexes and to validate the hVDRΔ structures, we used a VDR LBD from another species, the VDR of zebrafish. This paper describes

☆ Presented at the 12th Workshop on Vitamin D (Maastricht, The Netherlands, 6–10 July 2003).

* Corresponding author. Tel.: +33-3-88-653351; fax: +33-3-88-653276.
E-mail address: moras@igbmc.u-strasbg.fr (D. Moras).

0960-0760/$ – see front matter © 2004 Elsevier Ltd. All rights reserved.
doi:10.1016/j.jsbmb.2004.03.109

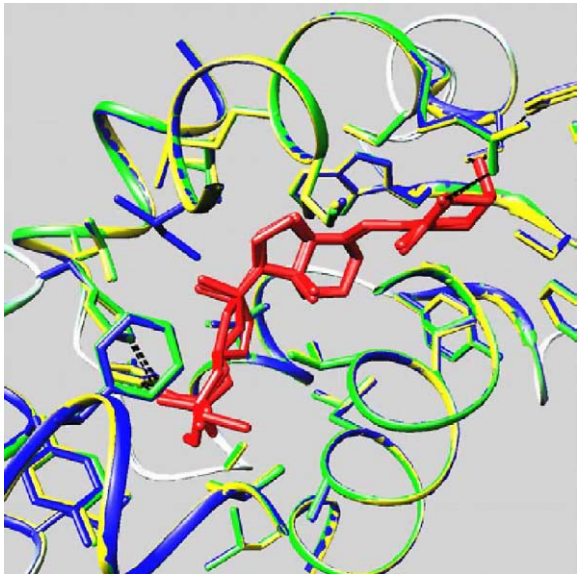

Fig. 1. Ligand binding pocket of the superimposed structures of hVDRΔ–1α,25(OH)$_2$D$_3$, hVDRΔ–KH1060, hVDRΔ–MC2100 complexes. The superimposed ligands are shown in red.

the purification and crystallization of the LBD of VDR of zebrafish bound to 1α,25(OH)$_2$D$_3$ and to Gemini.

2. Materials and methods

2.1. Expression and purification

The zebrafish VDR LBD (156-453) was cloned into the pET28b (Novagen) vector as hexahisdines-tagged protein and expressed in *E. coli* BL21 (DE3) (Novagen). A 200 ml LB preculture containing 200 μg kanamycin/ml was grown overnight at 37 °C and 25 ml aliquots of the preculture were used to inoculate 1 l LB culture containing 200 μg kanamycin/ml. Cells were grown at 37 °C to an absorbance at 600 nm of 0.6, and were allowed to grow for 12 h at 15 °C after induction by addition of 1mM IPTG (isopropyl β thiogalactoside). Cells were harvested by centrifugation and the pellets were frozen and kept at −80 °C. The cell pellet from 1 l culture was resuspended in 25 ml buffer containing 5 mM imidazole, 20 mM Tris pH 8.0, 250 mM NaCl, 5% glycerol, 1 mM PIC and 1 mM β-mercaptoethanol. The cells were lysed by sonication. The crude extract was loaded on an immobilized metal affinity column (Talon, Clontech) and eluted with imidazole. The fractions of interest were pooled and digested with bovine thrombine (1 unit per mg of protein) overnight at 4 °C in presence of 5 mM $CaCl_2$ to remove the histidine tag. The protein was loaded on a gel filtration Superdex 75 16/60 (Pharmacia) equilibrated in 10 mM Tris pH 7.0, 100 mM NaCl, 10 mM DTT (di-thio-threitol). The protein purity was analyzed by SDS-PAGE on a 12.5% polyacrylamide gel and Native-PAGE on an 8–25% gradient polyacrylamide gel and Coomassie blue staining. Protein concentration was determined by Bradford using BSA as standard. The protein was concentrated and incubated with a three-fold excess of ligand (1α,25(OH)$_2$D$_3$ or Gemini in ethanol) and SRC-1 peptide (686- RHKILHRLLQEGSPS-700).

2.2. Crystallization and X-ray data collection

Crystallization trials were carried out in 96 well plates on a TECAN robot using vapor-diffusion method. The crystals were then optimized in 24-well paltes by hanging drops diffusion method. Typically 3 μl of the concentrated protein was mixed with 3 μl of the reservoir solution and suspended from siliconized glass coverslips. Crystals were mounted in fiber loops and flash cooled in liquid ethane at liquid nitrogen temperature after cryoprotection with a solution containing the reservoir solution plus 5% glycerol and 2% polyethylene glycol 400. The data collection for the determination of the crystallographic parameters was performed at 100 K at the European Synchrotron Radiation Facility in Grenoble (beamline BM30) and at the Swiss Light Source (beamline PX). All data were integrated ans scaled using HKL2000 [15].

3. Results and discussion

Freshwater teleost zebrafish (*Danio rerio*) is a popular model for studying the roles of the various genes in development. Furthermore among the VDRs characterized so far, zebrafish, the second evolutionary most distant nuclear receptor from the human vertebrate, exhibits 100% identity in the LBP lining residues (Fig. 2). Its transactivation potency is 50% of that of hVDR [16]. This is consistent with other observations made with Xenopus VDR or lamprey VDR, which show 50% [9] and 25% [11] activity of the hVDR, respectively. The zVDR LBD exhibits 69% identity and 79% similarity in its sequence with the hVDR LBD, while the insertion region (191–252 of zVDR) exhibits only 34% identity and 47% similarity.

The optimization of the purification procedure led to the obtention of pure and homogenous protein in two chromatographic steps. The first affinity chromatography removed the majority of the contaminants and the second step, gel filtration, removed aggregates. The zVDR LBD behaves as a monomeric species on gel filtration. The protein was 95% pure as judged from the Coomassie stained gel (Fig. 3). One to two milligrams of pure protein for 1 l of culture were obtained. The first crystals were obtained from a screen on a TECAN crystallization robot. Then crystals of the complexes of zVDR LBD with 1α,25(OH)$_2$D$_3$ or Gemini were optimized at 24 °C using vapor diffusion in hanging drops. Reservoir solutions contained Bis–Tris 0.1 M pH 6.5, lithium sulfate 1.6 M and magnesium sulfate 50 mM. The crystals (Fig. 4) grew as hexagonal bipyramids of 200 μm × 100 μm × 100 μm within 2 days. Carefully

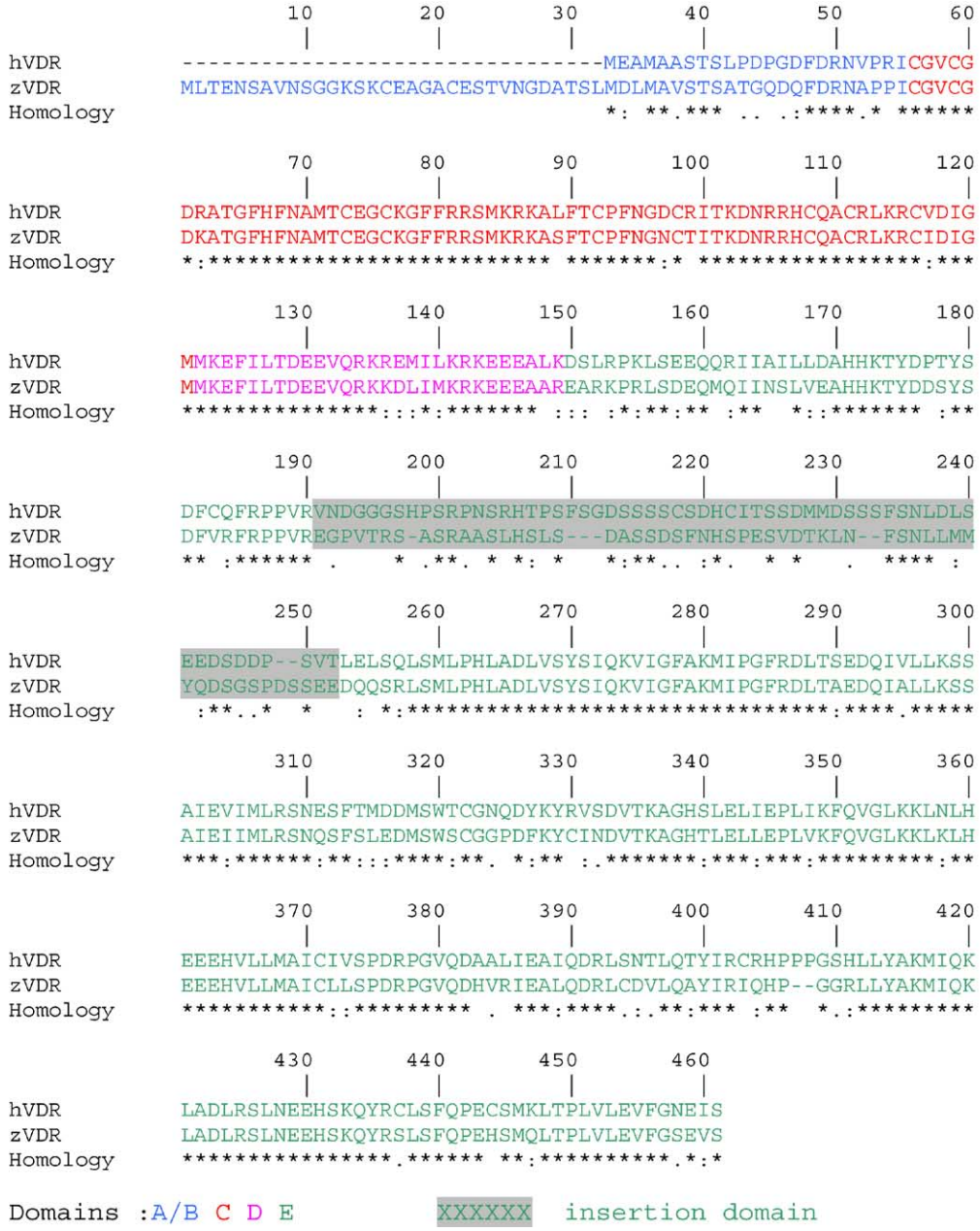

Fig. 2. Sequence alignment of zVDR vs. hVDR.

washed crystals were analyzed by SDS-PAGE to check the integrity of the protein in the crystals.

Crystals of zVDR-1α,25(OH)$_2$D$_3$ complex have a primitive hexagonal Laue lattice with unit cell parameters $a = b = 65.84$ Å and $c = 264.84$ Å. They diffract X-rays to a resolution limit of 2.2 Å. The systematic absences indicated either $P6_122$ or $P6_522$ space group. The data between 20 and 2.2 Å resolution was 99.0% complete with a Rsym of 4.8%. In the last resolution shell (2.28–2.20 Å) Rsym was 32.7 and the completeness was 99.5%. Initial phase estimates were obtained by molecular replacement using the structure of the hVDRΔ LBD as a starting model and a rigid body refinement to correctly position the molecule. The best solution indicate that the $P6_522$ was the correct space group. The program CNS-SOLVE [17] was used throughout structure determination and refinement calculations. The electron density are clear for all residues from the last two Histag residues to the C-terminal part except for the insertion region (191–252) and the last residue (453) which are missing in the final refinement. The model of zVDR-1α,25(OH)$_2$D$_3$ refined at 2.2 Å with a cutoff of 2σ comprises 234 residues (156–190; 253–452), 10 residues of the SRC-1 peptide (687–696), the ligand and 94 water molecules. The resulting refinement parameters are $R = 22.0\%$ and Rfree $= 25.1\%$. For the crystals of the complex of zVDR-Gemini, the space group is $P6_522$ with the unit cell parameters $a = b = 65.86$ Å and

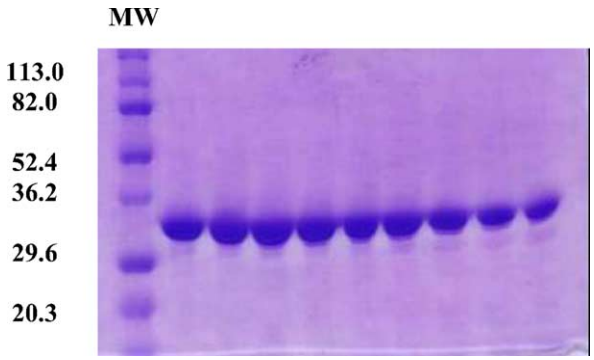

Fig. 3. Coomassie stained SDS gel of the zVDR LBD gel filtration fractions corresponding to the peak. MW molecular markers in kDa.

$c = 265.02$ Å. The data between 20 and 2.6 Å resolution was 85.5% complete with a Rsym of 4.2%. In the last resolution shell (2.69–2.60 Å) Rsym was 19.1 and the completeness was 68.5%. The final model of zVDR-Gemini refined at 2.6 Å with a cutoff of 2σ comprises 234 residues (156–190; 253–452), 10 residues of the SRC-1 peptide (687–696), the ligand and 38 water molecules, and the refinement parameters are $R = 20.4\%$ and Rfree $= 26.0\%$.

The zVDR LBD is in the canonical active conformation and binds to the SRC-1 peptide in the classical way [18] (Fig. 5). The structures of the zVDR and hVDRΔ LBDs are similar with a root mean square deviation of 0.72 Å over 236 main chain atoms. The insertion region deleted in the hVDRΔ construct and present in the crystals of zVDR LBD is not visible in the electron density map reflecting its disorder. Helix H3*n* observed in the hVDR structure is missing in the zVDR. The binding pocket is identical and the natural ligand adopts the same conformation and forms the same interactions with the protein in the two structures. This structure of a wild-type VDR thus validates our previous conclusions made on the hVDRΔ structures.

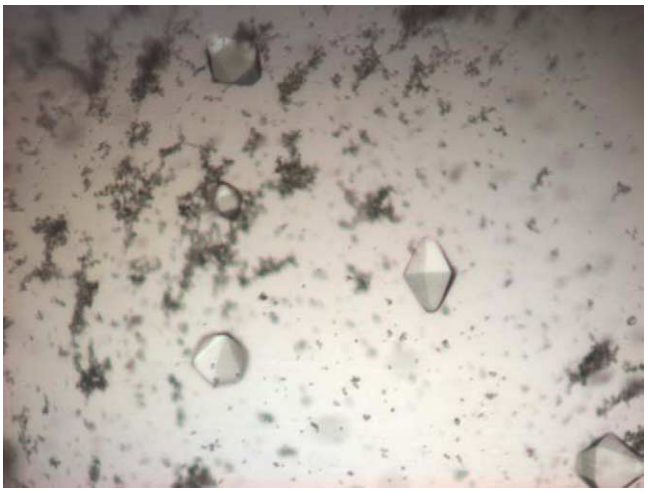

Fig. 4. Crystals of zVDR–1α,25(OH)$_2$D$_3$. The crystals were obtained in Bis–Tris 0.1 M pH 6.5, lithium sulfate 1.6 M and magnesium sulfate 50 mM. The size of the largest crystals were 200 μm × 100 μm × 100 μm.

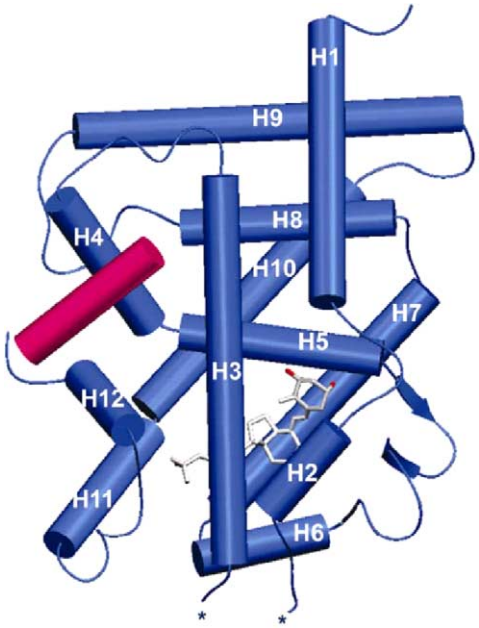

Fig. 5. Overall view of the structure of zVDR LBD–1α,25(OH)$_2$D$_3$. The VDR is shown in blue and the SRC-1 peptide in pink. The ligand is shown in gray with the oxygen atoms in red. The zVDR missing loop ends are marked by stars.

An additional important advantage of this new crystal packing is that the most flexible part of the LBD that involves the loop H2–H3 notably H3*n* in hVDRΔ crystal structure is not involved in the crystal packing interactions. Any conformational change that would affect this part of the protein does not prevent crystallization. Therefore we used this new crystal form to screen the crystallization of several complexes and obtain crystals of the zVDR bound to Gemini, an interesting ligand with two identical side chains at carbon C20 [19]. This ligand with an unusual stereochemistry shows a 25% increase in volume compared to the natural ligand. In this complex, the protein adapts to the synthetic ligand while preserving the agonist conformation. Fig. 6 shows the

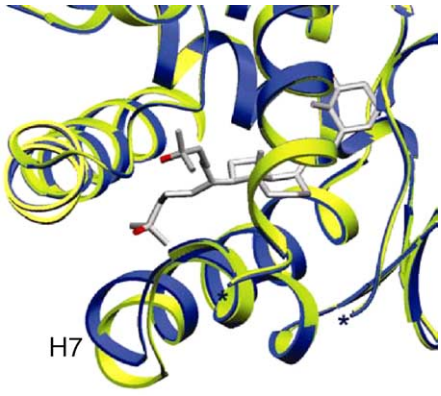

Fig. 6. Superimposition of the zVDR LBD–1α,25(OH)$_2$D$_3$ (blue) and the zVDR LBD-Gemini (green) in the region differing the most. The Gemini is shown in gray with the oxygen atoms in red. The zVDR missing loop ends are marked by stars.

superimposition of the zVDR structures in the region differing the most, together with the Gemini ligand. The presence of a second side chain induces a rearrangement of the beginning of H7 leading to the formation of a new pocket. One of the side chain takes the place of the side chain of the natural ligand while the second side chain points towards H7 and the end of H10. This mutual adaptation of the protein and the ligand confirms the induced-fit mechanism of ligand binding.

Acknowledgements

We are grateful to A. Steinmeyer (Schering AG) for a generous gift of $1\alpha,25(OH)_2D_3$ and F. Bjoerkling (Leo Pharmaceutical Products) and M.R. Uskokovic (BioXell) for providing us with Gemini. We thank the beamline staff at the European Synchrotron Radiation Facility (ESRF, Grenoble, France) and at the Swiss Light Source (SLS, Villigen, Switzerland) for technical assistance during data collection. We thank V. Chavant and F. Zink for crystallization trials on TECAN robot and L. Brondani for technical assistance. This work was supported by grants from CNRS, INSERM and Ministère de la Recherche et de la Technologie. This work benefits from the technical plateform of structural genomics supported by the Genopole and SPINE programs.

References

[1] D.J. Mangelsdorf, C. Thummel, M. Beato, P. Herrlich, G. Schutz, K. Umesono, B. Blumberg, P. Kastner, M. Mark, P. Chambon, et al., The nuclear receptor superfamily: the second decade, Cell 83 (1995) 835–839.

[2] E. Kalkhoven, J.E. Valentine, D.M. Heery, M.G. Parker, Isoforms of steroid receptor co-activator 1 differ in their ability to potentiate transcription by the oestrogen receptor, EMBO J. 17 (1998) 232–243.

[3] C. Rachez, B.D. Lemon, Z. Suldan, V. Bromleigh, M. Gamble, A.M. Naar, H. Erdjument-Bromage, P. Tempst, L.P. Freedman, Ligand-dependent transcription activation by nuclear receptors requires the DRIP complex, Nature 398 (1999) 824–828.

[4] R. Bouillon, W.H. Okamura, A.W. Norman, Structure-function relationships in the vitamin D endocrine system, Endocr. Rev. 16 (1995) 200–257.

[5] A.R. Baker, D.P. McDonnell, M. Hughes, T.M. Crisp, D.J. Mangelsdorf, M.R. Haussler, J.W. Pike, J. Shine, B.W. O'Malley, Cloning and expression of full-length cDNA encoding human vitamin D receptor, Proc. Natl. Acad. Sci. U.S.A. 85 (1988) 3294–3298.

[6] J.K. Burmester, R.J. Wiese, N. Maeda, H.F. DeLuca, Structure and regulation of the rat 1,25-dihydroxyvitamin D3 receptor, Proc. Natl. Acad. Sci. U.S.A. 85 (1988) 9499–9502.

[7] Y. Kamei, T. Kawada, T. Fukuwatari, T. Ono, S. Kato, E. Sugimoto, Cloning and sequencing of the gene encoding the mouse vitamin D receptor, Gene 152 (1995) 281–282.

[8] Z. Lu, K. Hanson, H.F. DeLuca, Cloning and origin of the two forms of chicken vitamin D receptor, Arch. Biochem. Biophys. 339 (1997) 99–106.

[9] Y.C. Li, C. Bergwitz, H. Juppner, M.B. Demay, Cloning and characterization of the vitamin D receptor from Xenopus laevis, Endocrinology 138 (1997) 2347–2353.

[10] T. Suzuki, N. Suzuki, A.S. Srivastava, T. Kurokawa, Identification of cDNAs encoding two subtypes of vitamin D receptor in flounder, Paralichthys olivaceus, Biochem. Biophys. Res. Commun. 270 (2000) 40–45.

[11] G.K. Whitfield, H.T. Dang, S.F. Schluter, R.M. Bernstein, T. Bunag, L.A. Manzon, G. Hsieh, C. Encinas Dominguez, J.H. Youson, M.R. Haussler, J.J. Marchalonis, Cloning of a functional vitamin D receptor from the lamprey (Petromyzon marinus), Endocrinology 144 (2003) 2704–2716.

[12] N. Rochel, J.M. Wurtz, A. Mitschler, B. Klaholz, D. Moras, The crystal structure of the nuclear receptor for vitamin D bound to its natural ligand, Mol. Cell 5 (2000) 173–179.

[13] N. Rochel, G. Tocchini-Valentini, P.F. Egea, K. Juntunen, J.M. Garnier, P. Vihko, D. Moras, Functional and structural characterization of the insertion region in the ligand binding domain of the vitamin D nuclear receptor, Eur. J. Biochem. 268 (2001) 971–979.

[14] G. Tocchini-Valentini, N. Rochel, J.M. Wurtz, A. Mitschler, D. Moras, Crystal structures of the vitamin D receptor complexed to superagonist 20-epi ligands, Proc. Natl. Acad. Sci. U.S.A. 98 (2001) 5491–5496.

[15] Z. Otwinowski, W. Minor, Processing X-ray data collected in oscillation mode, Methods Enzymol. 276 (1997) 307–326.

[16] A. Kouzmenko, Personal communication.

[17] A.T. Brunger, P.D. Adams, G.M. Clore, W.L. DeLano, P. Gros, R.W. Grosse-Kunstleve, J.S. Jiang, J. Kuszewski, M. Nilges, N.S. Pannu, et al., Crystallography & NMR system: a new software suite for macromolecular structure determination, Acta Crystallogr. D: Biol. Crystallogr. 54 (1998) 905–921.

[18] B.D. Darimont, R.L. Wagner, J.W. Apriletti, M.R. Stallcup, P.J. Kushner, J.D. Baxter, R.J. Fletterick, K.R. Yamamoto, Structure and specificity of nuclear receptor-coactivator interactions, Genes Dev. 12 (1998) 3343–3356.

[19] A.W. Norman, P.S. Manchand, M.R. Uskokovic, W.H. Okamura, J.A. Takeuchi, J.E. Bishop, J.I. Hisatake, H.P. Koeffler, S. Peleg, Characterization of a novel analogue of 1alpha,25(OH)(2)-vitamin D(3) with two side chains: interaction with its nuclear receptor and cellular actions, J. Med. Chem. 43 (2000) 2719–2730.